Lawrence Berkeley National Laboratory
Recent Work

Title

PHOTON INDUCED X-RAY FLUORESCENCE ANALYSIS USING ENERGY DISPERSIVE DETECTOR and DICHOTOMOUS SAMPLER

Permalink

https://escholarship.org/uc/item/89t5p89g

Author

Jaklevic, J.M.

Publication Date

1976

LBL-4834

c.1

PHOTON INDUCED X-RAY FLUORESCENCE ANALYSIS USING
ENERGY DISPERSIVE DETECTOR AND DICHOTOMOUS SAMPLER

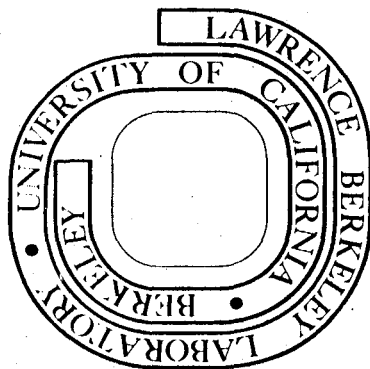J. M. Jaklevic, B. W. Loo, and F. S. Goulding

January 1976

LBL-4834

c.1

DISCLAIMER

PHOTON INDUCED X-RAY FLUORESCENCE ANALYSIS
USING ENERGY DISPERSIVE DETECTOR AND DICHOTOMOUS SAMPLER*

J. M. Jaklevic, B. W. Loo and F. S. Goulding

Lawrence Berkeley Laboratory
University of California
Berkeley, California 94720 U.S.A.

INTRODUCTION

In recent years X-ray fluorescence analysis has emerged as a very power-
ful technique for the elemental analysis of environmental samples. Several
laboratories are currently applying the technique to the analysis of air-
borne particulate matter. The samples typically consist of uniform deposits
of particulate matter collected on a thin clean substrate making them ideally
suited for non-destructive X-ray analysis.

Traditionally X-ray tubes have been employed to excite the fluorescence
in samples and crystal spectrometers were used to disperse and analyze the
characteristic X-rays according to their wavelength. The development of semi-
conductor detectors has made possible the use of energy-dispersive spectrom-
eters together with either heavy charged particle or photon excitation. The
charged particles are typically 3 MeV protons or 16 MeV alpha particles which
have been generated by an accelerator. Alternatively, photon excitation by
monochromatic or broadband X-rays generated either in a X-ray tube or radio-
isotope source can be used.

Energy-dispersive analysis with charged particle excitation and wave-
length-dispersive analysis are discussed in Chapters 2 and 3 of this book.
We shall describe an energy dispersive X-ray fluorescence system using photon
excitation which has been designed for a large-scale aerosol sampling network.
In addition to providing the required sensitivity for air particulate analysis,
the X-ray unit has been designed for fully automatic operation as an integral
part of a complete sampling, analysis, and data handling system. An automatic
air sampler has been developed capable of acquiring particle size-segregated
aerosol specimens which are compatible with the X-ray fluorescent unit. This
discussion of the complete system is limited by the scope of the present
paper; previous publications give a more complete description of the techniques
employed.[1-5]

X-RAY FLUORESCENCE SYSTEM BASIC CONCEPTS

A simplified schematic of an X-ray fluorescence technique is shown in Fig. 1. Primary radiation is incident on the sample where it interacts to produce vacancies in the inner atomic shells which then deexcite to produce the characteristic X-rays of interest. These X-rays from the sample are then detected, and their energies are measured by the semiconductor detector spectrometer.

The semiconductor detector spectrometer converts the energy of the incident X-ray into a voltage pulse whose amplitude is proportional to that energy. A multichannel analyzer is used to accumulate a histogram of the pulse amplitude spectrum. The energy resolution of the semiconductor detector spectrometer is more than adequate to separate X-ray lines from elements of adjacent atomic numbers. As such, it is capable of performing simultaneous multiple element analysis for typical aerosol samples. The area of the individual characteristic X-ray peaks in the spectrum is proportional to the concentration of the various elements in the sample.

DESIGN OF EXCITATION SYSTEMS

An X-ray tube was chosen as the primary excitation source because of its higher output compared to generally available radioisotope sources. The requirement to analyze 100 or more samples per day requires the highest possible counting rate. Photons incident on the sample interact either by the photoelectric effect to produce the desired inner-shell atomic vacancies in the elements of interest or by scattering mainly from the atoms in the low atomic number substrate. These scattered X-rays constitute an unwanted background which set the detection limit for the fluorescence measurement.

Figure 2 is a schematic of a spectrum produced by monoenergetic X-rays exciting a low atomic number filter substrate containing a few trace elements. The coherent (Rayleigh) and incoherent (Compton) scattering peaks occur at or just below the energy of the incident X-rays. For good sensitivity the fluorescent X-rays of the elements must not overlap the scatter peaks. This effect favors the use of monoenergetic X-ray excitation sources rather than broadband excitation which would distribute the scattered radiation over the

entire range of energies. However, the probability of producing fluorescent excitation of an element is greatest when the exciting X-ray energy just exceeds the binding energy of the electrons in the appropriate shells and falls off rapidly with increasing excitation energy. This implies that very low energy characteristic X-rays are not efficiently produced by monochromatic radiation of high energy, thus limiting the range of elements which can be sensitively measured with a single exciting energy. This effect compensates for some of the disadvantages of continuous excitation cited earlier. In some cases, such as the analysis for very light elements (Z < 20), the use of continuum excitation may give better sensitivity than monochromatic excitation.

In order to cover as broad a range of elements as possible with optimum excitation we have chosen to employ three measurements on each sample using a different X-ray excitation energy for each. This is accomplished by operating in a secondary fluorescence mode in which the continuum radiation from the X-ray tube anode is incident on a secondary target whose characteristic X-rays are then used to irradiate the sample. This method of generating nearly mono-energetic X-ray excitation has the advantage that it can be performed exter-nally by mechanically switching the secondary target.

Figure 3 shows a cross section of the fluorescence geometry. The secondary target is in the form of a sheet metal enclosure which is moved as a integral assembly with the collimators. The secondary targets, principle excitation energies, and range of atomic numbers analyzed by each are as follows:

i)   Ti,   4.5 keV, $13 \leqslant Z \leqslant 20$,

ii)   Mo,   17.4 keV, $20 \leqslant Z \leqslant 38$ together with the L X-rays for heavy elements
        Pb and Hg,

iii)   Tb,   44 keV, $38 \leqslant Z \leqslant 56$.

The X-ray tube is of a special design that projects the electron beam through a narrow tube onto a grounded anode. This allows for a tight geometry between secondary targets and the sample. Using this close coupled geometry we achieve maximum counting rates (15,000 counts/sec) with a X-ray tube power dissipation well below 100 watts.

DETECTOR CONSIDERATIONS

A low-background guard-ring detector is used in the spectrometer to ensure low background in the region below the scatter peaks.[6] A pulsed-light feedback electronic system is used to provide good energy resolution and high counting rate capabilities. Of particular interest in our most recent X-ray fluorescence system is the use of a pulsed X-ray tube to provide a greatly increased output counting rate. In this system an X-ray tube control grid is operated in a feedback loop with the detector output in such a way that the tube is pulsed off when the electronics is processing a signal and turned on only when the system is prepared to analyze an event.[7] The effective output counting rate can be increased two to three times using this method while still limiting pulse pile-up to a tolerable value.

SAMPLE FORM AND CALIBRATION

The present system has been designed to accommodate air-particulate samples collected by filtration. These samples consist of a thin, uniform deposit of particles collected on clean membrane filters consisting of cellulose, poly-carbonate, or other hydrocarbons. Glass fiber filters generally contain substantial amounts of elemental contaminates which interfere with the analysis and are not suitable for these applications.

The calibration of the X-ray analyzer consists of converting the observed characteristic X-ray counting rates to concentration of elements expressed as ng/cm^2 on the filter. A simple model can be used to describe the relative efficiency for detecting X-rays as a function of concentration of a given element. For samples in which the attenuation of the fluorescence X-rays can be neglected, the counting rate for a given characteristic X-ray can be expressed as

$$I_i = I_o \, G \, K_i \, \rho_i$$

where I_o is the X-ray source intensity, G is a geometry and efficiency factor, ρ_i is the concentration of element i, and K_i is the relative X-ray excitation

cross-section.   In this simple case and when using monoenergetic excitation, K_i can be calculated from a straightforward physical model of X-ray photo-electron interactions.[8]

In cases where the X-ray energies are low enough that absorption either within the filter matrix or from the individual particles becomes important, an added attenuation correction must be included.   It is the magnitude of this correction and the ability to estimate it accurately which constitutes the major limitation of the XRF technique in the case of light elements.   Several papers discussing both this problem and calibration techniques in general are included in this volume.

Figure 4 illustrates the operation of the X-ray fluorescence system in a completely automatic mode for large-scale analysis applications.   The aerosol samples are collected on membrane filters mounted in a standard 5 cm x 5 cm holder which is compatible with the standard 35 mm slide projector hardware used in the automatic sample handling.   An automatic stack loader is used to sequence the samples through the analysis system.   The operation of the stack loader, secondary target manipulation, and X-ray tube controller is sequenced by a central control unit programmed by a small computer.   The computer is also used as a pulse height analyzer and data output controller.   A spectrum analysis program is included in the computer software and the data are written on the output tape both in its original spectral form and reduced to concentra-tion per unit area.[1,5]   The output data are subsequently corrected for filter attenuation, particle size and possible interelement effects before being stored in a data bank.[9,10]

AIR SAMPLER DESIGN

Routine collection of aerosol particles on a membrane type filter is a straightforward problem requiring that a known volume of air be drawn through the filter using a vacuum pump.   Flow rates of 5 to 10 $\ell/min/cm^2$ of the fil-ter can easily be achieved.   At this rate it is possible to observe major ele-mental constituents of the urban aerosol in samples of 30 min or less.   More typically, samples are acquired in 2 to 6 hours or longer depending upon the nature of the monitoring problem.

Recent air sampling requirements have emphasized the collection of particulate samples each representing a different particle size fraction of the aerosol. In particular, it is important to collect the two major components of the bimodal urban aerosol[11] as separate samples. It has been established that the fine particle accummulation mode with a peak at about 0.3 μm mass median diameter consists primarily of the combustion products while natural and mechanically generated aerosols are usually over several microns in size. A size cut at about 2 μm corresponding to the minimum in the bimodal volume or mass distribution not only separates the particles according to their origin, and hence chemical properties, but also renders the procedure for X-ray attenuation corrections more manageable.

The most widely used sampling technique for acquiring size segregated particles involves the removal of the particles from the air stream by impaction on a plate. Figure 5 illustrates a typical impactor stage. The air is directed through a narrow slit onto an opposing surface causing the streamlines to turn abruptly. Particles in the air stream experience the opposing forces of the viscous interaction in the air and the inertial tendency to travel in a straight line. The viscous force is proportional to the cross sectional area of the particle whereas the inertia 'force' is proportional to the particle volume. By suitably adjusting the air velocity and average turning radius particles above a certain effective diameter are caused to impact onto the plate while the smaller particles remain in the air stream. A number of commercially available air samples utilize this process to collect samples in a sequence of successively smaller particle size ranges.

This method possess several disadvantages with respect to subsequent X-ray fluorescence analysis. Patterns of particle depositions are images of the narrow slits used in the individual impactor stage. Such small area, high density deposits do not satisfy the criteria for uniformity and thickness established earlier. The conventional impactor also exhibits certain inherent disadvantages. Particles incident on the impaction surface often fail to adhere and become re-entrained in the air flow. This 'particle bounce' phenomenon results in large particles being collected in the smaller particle fraction. In the case where heavy deposits are accumulated on the impaction surface, the surface particles can be blown off by the air stream and recollected by a later stage.

To avoid these problems and to provide aerosol specimens suitable for XRF analysis, we have designed an air sampler based on the principle of virtual impaction.[4] Instead of a physical plate for an impaction surface, the aero-dynamics are designed such that the 'impaction' occurs into a separate air volume which can then be drawn through a filter. Figure 6 illustrates a single circular jet which is 'impacted' into a tube with a portion of the flow Q_1 drawn into the tube with a majority of the flow Q_2 continuing around the impaction tube. The large particles should remain in the flow Q_1 whereas the small particles will be divided between Q_1 and Q_2 in proportion to the relative air flows. It is obvious that such a design is free from the problem of particle bounce and flow-off and, in fact, turns these effects to its advantage.

Following an extensive program of measuring the properties of such an impactor stage, we have designed a two-stage virtual impactor with a single cut point at 2.4 µm particle diameter. This 'dichotomous' air sampler operates at an input flow rate of 50 ℓ/min; the outputs of the device are passed through a pair of membrane filters similar to those discussed earlier. Figure 7 shows a schematic of the flow through the system. To ensure stable operating conditions, the flow division Q_1/Q_2 and total flow Q_0 are maintained constant by monitoring the pressure drop across the fixed orifice in the system. This compensates for any change in flow caused by the increased loading on the membrane. Figure 8 shows the effectiveness of the size separation process. The fraction A/A+B is the fraction of particles which are collected as large particles. The fraction of particles lost through the impaction on various inner surfaces is also shown. The solid particle losses have been reduced to a tolerable level which compares favorably with the performance of other types of air samplers.

An automatic air sampler incorporating the dichotomous virtual impactor as a first stage has been designed and ten such units have been operating in St. Louis for the past year. The sampler accommodates the membrane filter holder in pairs which are automatically sequenced according to a predetermined sampling schedule. The 5 cm x 5 cm samples are contained in conventional 36 slide cartridges used in photographic slide projectors. These cartridges are changed as needed and returned to a central laboratory for analysis by X-ray fluorescence.

Also included in the program is a total mass measurement using a beta-particle attenuation method.[3] The filters are gauged before and after exposure to the aerosol and the mass difference measured. Such mass differences can be measured to an overall accuracy of $\pm$ 10 $\mu g/cm^2$ with 30 second measurements.

RESULTS

Figures 9 and 10 illustrate X-ray fluorescence data taken on a pair of filters which were exposed in the automatic dichotomous sampler. The difference in elemental distribution from the two particle-size ranges is apparent. The elements Pb and Br are predominantly in the small particle fraction, whereas Ca and Fe are mostly contained in the large particles. The small aerosol particles (< 2 μm diameter) are assumed to originate from combustion reactions such as automotive engines for Pb and Br. The large particles originate from mechanical processes such as wind blown soil dust.[12,13]

Analysis of this type of data from a time sequence of samples exposed at several sites yields information on the time and spatial variation of elemental contaminants in the atmosphere. During the past year over 15,000 such samples have been collected using automatic dichotomous samplers at ten selected sites in the St. Louis area. These are currently being analyzed using photon-excited energy-dispersive analysis and data are being incorporated into the EPA Regional Air Pollution Study (RAPS) data bank.

Figures 11 and 12 show plots of fine and coarse particle concentrations for the elements S and Pb in air samples taken over a period of three days beginning on July 29, 1975. The fact that S and Pb appear predominantly in the fine particle fraction indicates that their origin is in combustion processes from fossil fuel power plants (S) and automotive exhaust (Pb). The difference in diurnal patterns for the data acquired at an urban sampling station (BAPS site 103) reflects the periodic behavior of automobile traffic patterns in the Pb concentration as opposed to the slowly varying S levels. A graph of the concentration as a function of the site shows the variation of concentration over a 40 km radius of downtown St. Louis. The behavior of the

sulfur concentration indicates a widespread background level over the entire region whereas the Pb concentration reflects the local traffic densities at the sampling sites. For example, RAPS sites 122 and 124 are in relatively remote rural areas approximately 40 km from St. Louis whereas sites 105, 106, 112 and 120 are in the St. Louis urban area.

CONCLUSION

Operating experience in using the photon-excited energy-dispersive X-ray fluorescence analysis system has demonstrated the applicability of this technique to large-scale air-sampling networks. This experience has shown that it is possible to perform automatic sampling and analysis of aerosol particulates at a sensitivity and accuracy more than adequate for most air pollution studies.

ACKNOWLEDGEMENTS

The authors wish to express their appreciation to the other members of the group who have contributed to the design, construction and operation of the aerosol analysis sytem. These include R. Gatti, B. Jarrett, D. Landis, N. Madden, J. Meng and W. Searles. T. Dzubay of the Environmental Protection Agency has contributed much in the way of technical advice and encouragement during the course of this program.

REFERENCES

1.   Goulding, F. S. and J. M.Jaklevic. "X-Ray Fluorescence Spectrometer for Airborne Particulate Monitoring", EPA Report No. EPA-R2-73-182 (1973).

2.   Goulding, F. S. and J. M.Jaklevic. "Development of Air Particulate Monitoring Systems", EPA Report No. EPA-650-4-74-030 (1974).

3.   Goulding, F. S., Jaklevic, J. M. and B. W. Loo. "Fabrication of Monitoring System for Determining Mass and Composition of Aerosols as a Function of Time", EPA Report No. EPA-650/2-75-048 (1975).

4.   Loo, B. W., Jaklevic, J. M. and F.'S. Goulding. "Dichotomous Virtual
     Impactors for Large Scale Monitoring of Airborne Particulate Matter",
     in Fine Particles: Aerosol Generation, Measurement, Sampling and Analysis,
     B. Y. H. Liu, Ed. (New York, New York: Academic Press, 1976) pp. 311-350.

5.   Jaklevic, J. M., Goulding, F. S., Jarrett, B. V. and J. D. Meng. In
     Analytical Methods Applied To Air Pollution Measurements, R. K. Stevens
     and W. F. Herget, Eds. (Ann Arbor, Michigan: Ann Arbor Science Publishers,
     Inc. 1974), p. 123.

6.   Goulding, F. S., Jaklevic, J. M., Jarrett, B. V. and D. A. Landis.
     "Detector Background and Sensitivity of X-ray Fluorescence Spectrometers",
     Adv. X-ray Anal., 15, 470 (1972).

7.   Jaklevic, J. M., Landis, D. A. and F. S. Goulding. "Energy Dispersive
     X-ray Fluorescence Spectrometry Using Pulsed X-ray Excitation", Adv.
     X-ray Anal., 19, 253 (1976).

8.   Giauque, R. D., Goulding, F. S., Jaklevic, J. M. and R. H. Pehl. "Trace
     Element Determination With Semiconductor Detector X-ray Spectrometers",
     Anal. Chem., 45, 671 (1973).

9.   Dzubay, T. G. and R. O. Nelson. "Self Absorption Corrections for X-ray
     Fluorescence Analysis of Aerosols", Adv. X-ray Anal., 18, 619 (1975).

10. Loo, B. W., Gatti, R. C., Liu, B. Y. H., Kim, C. and T. G. Dzubay.
     "Absorption Corrections for Submicron Sulfur Collected in Filters", in
     X-Ray Fluorescence Analysis of Environmental Samples, Chap. ___, T. G.
     Dzubay, Ed. (Ann Arbor, Michigan: Ann Arbor Science Publishers, Inc.
     1976).

11. Whitby, K. T., Husar, R. B. and B. Y. H. Liu. "The Aerosol Size Distribu-
     tion of Los Angeles Smog", in Aerosols and Atmospheric Chemistry, G. M.
     Hidy, Ed. (Academic Press, 1972) pp. 237-264.

12. Dzubay, T. G. and R. K. Stevens. Envir. Sci. Technol., 9, 663 (1975).

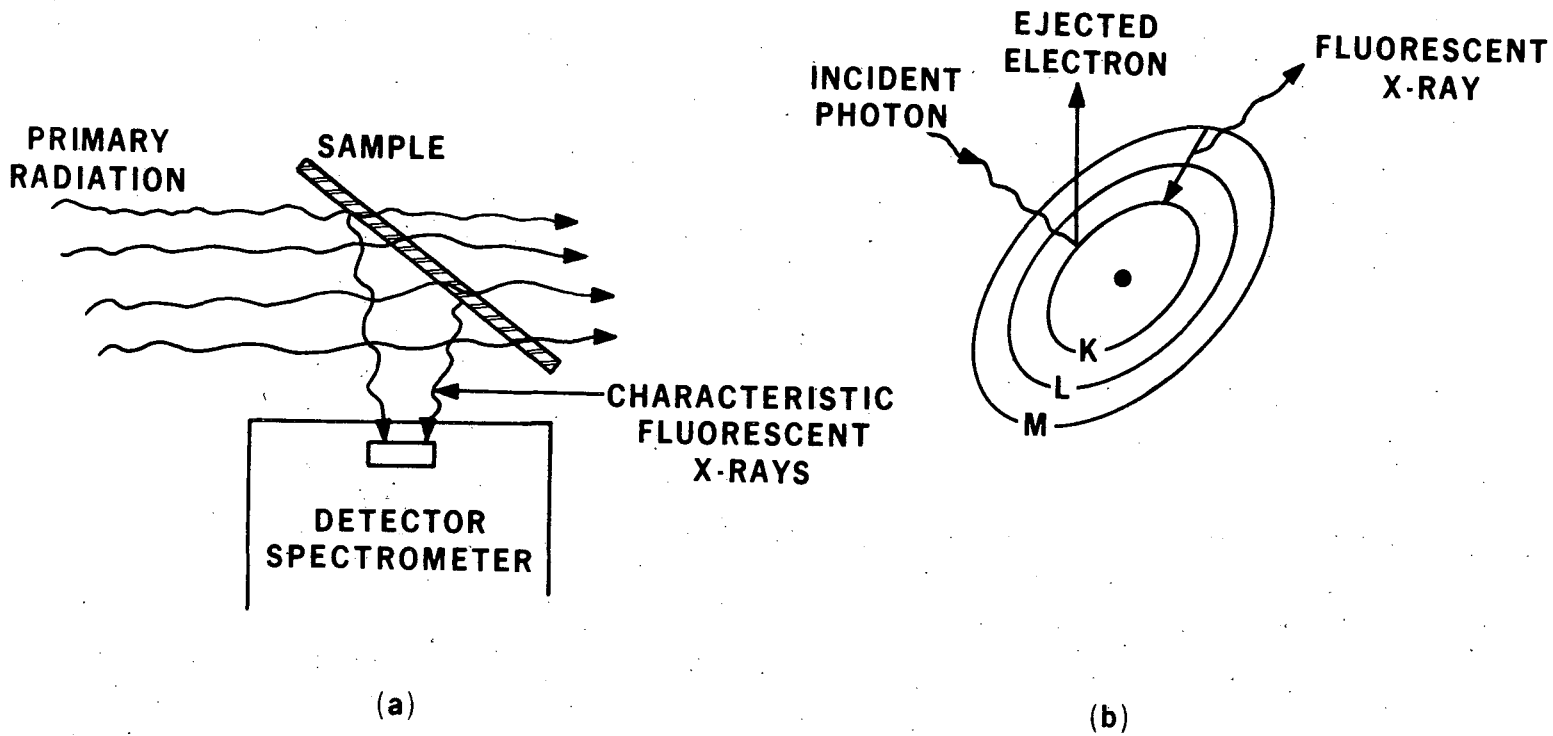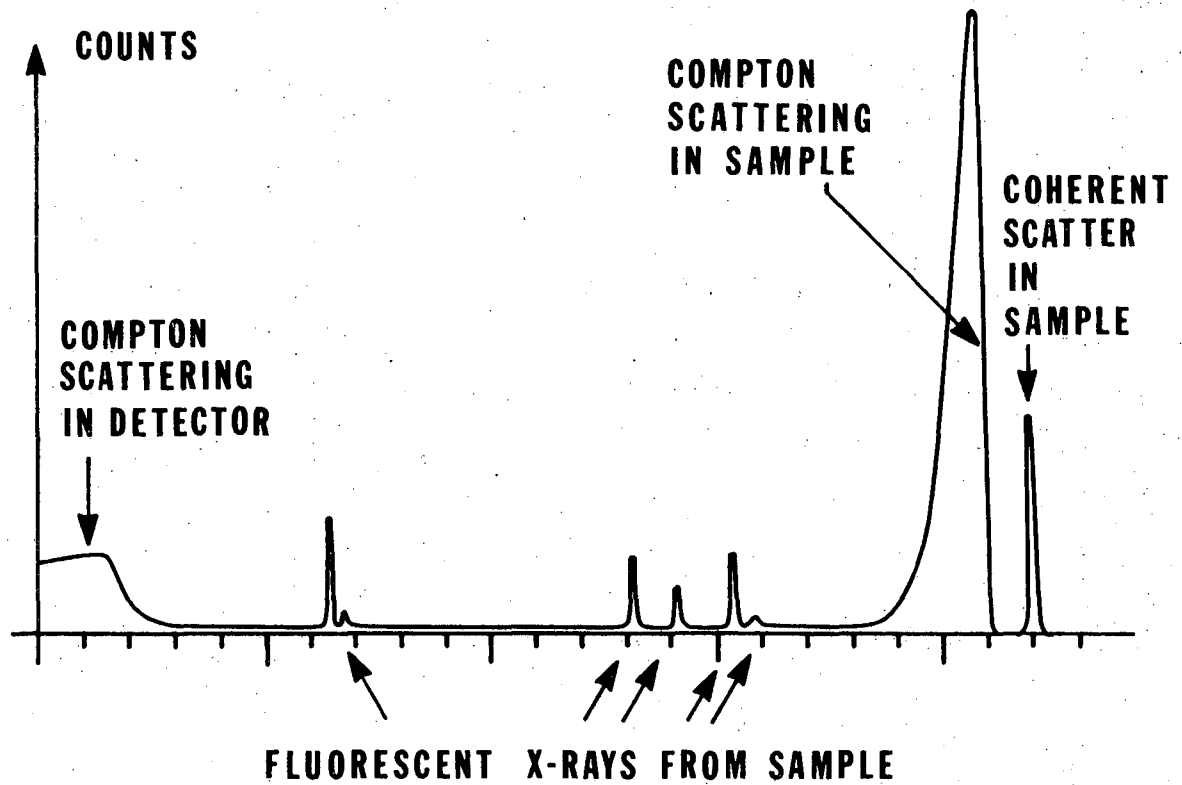13. Friedlander, S. K.   Envir. Sci. Technol., 7, 1115 (1973).

FIGURE CAPTIONS

Figure 1. Schematic of the X-ray fluorescence technique.

Figure 2. The response of the spectrometer for monoenergetic photons
           striking the sample. The matrix is assumed to be composed
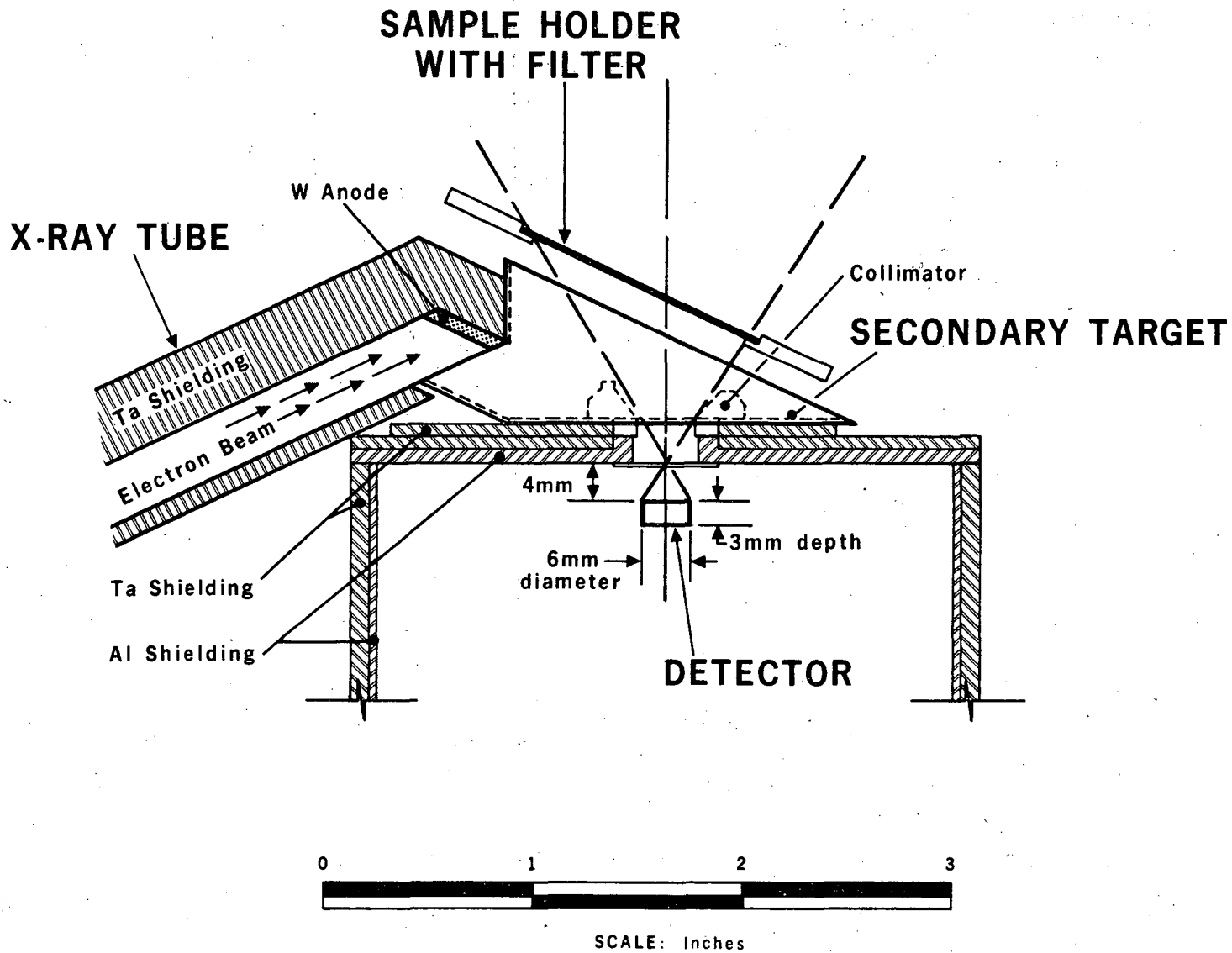   of light elements.

Figure 3. Sample - Fluorescer - Detector geometry employed in the
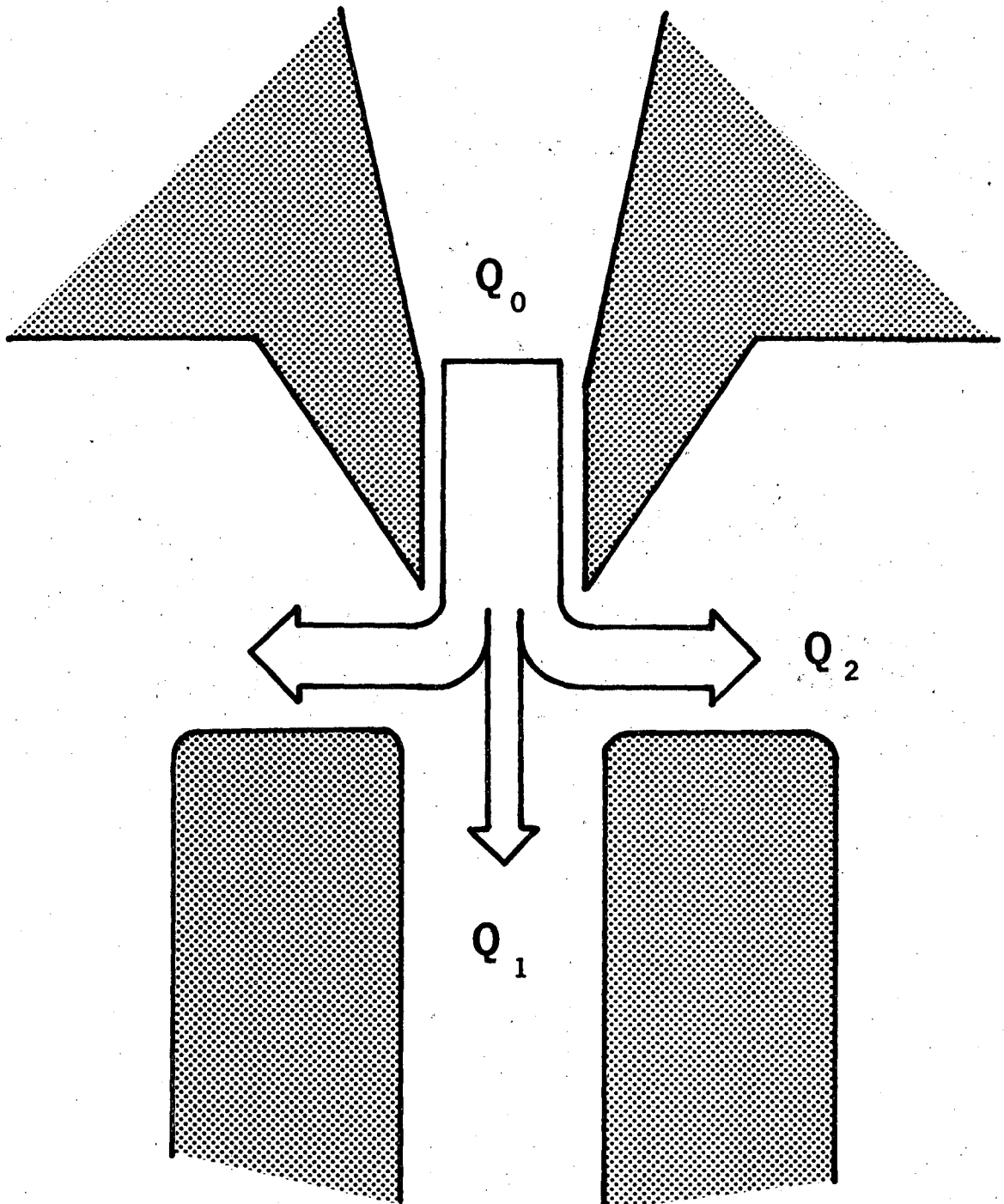   secondary fluorescence mode of energy dispersive analysis.
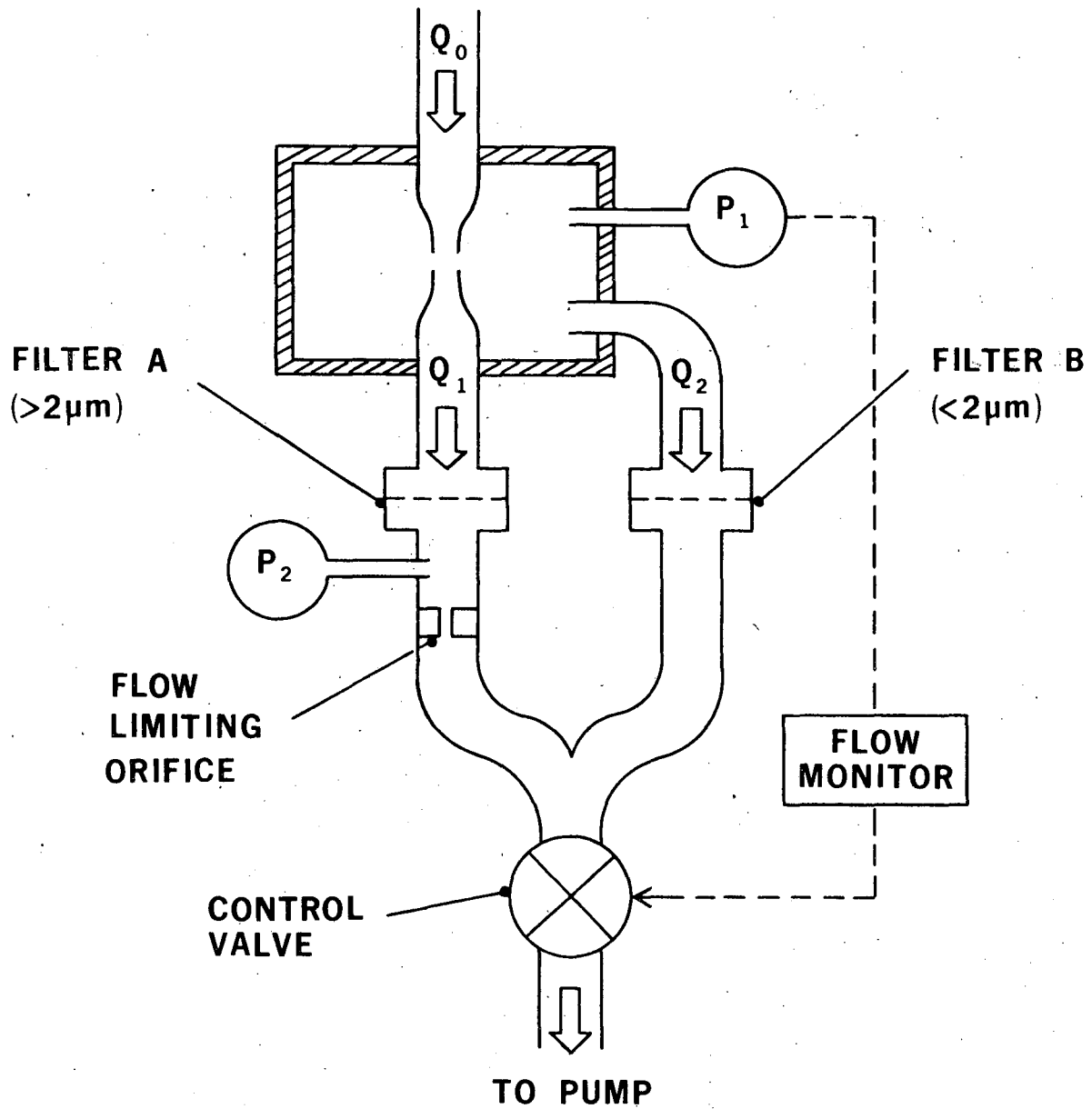
Figure 4. Block diagram of complete analysis system.

Figure 5. Schematic of a single impactor stage.

Figure 6. Schematic of a virtual impaction orifice.

Figure 7. Flow diagram for a dichotomous virtual impactor. Filters
           A and B are membrane type filters.
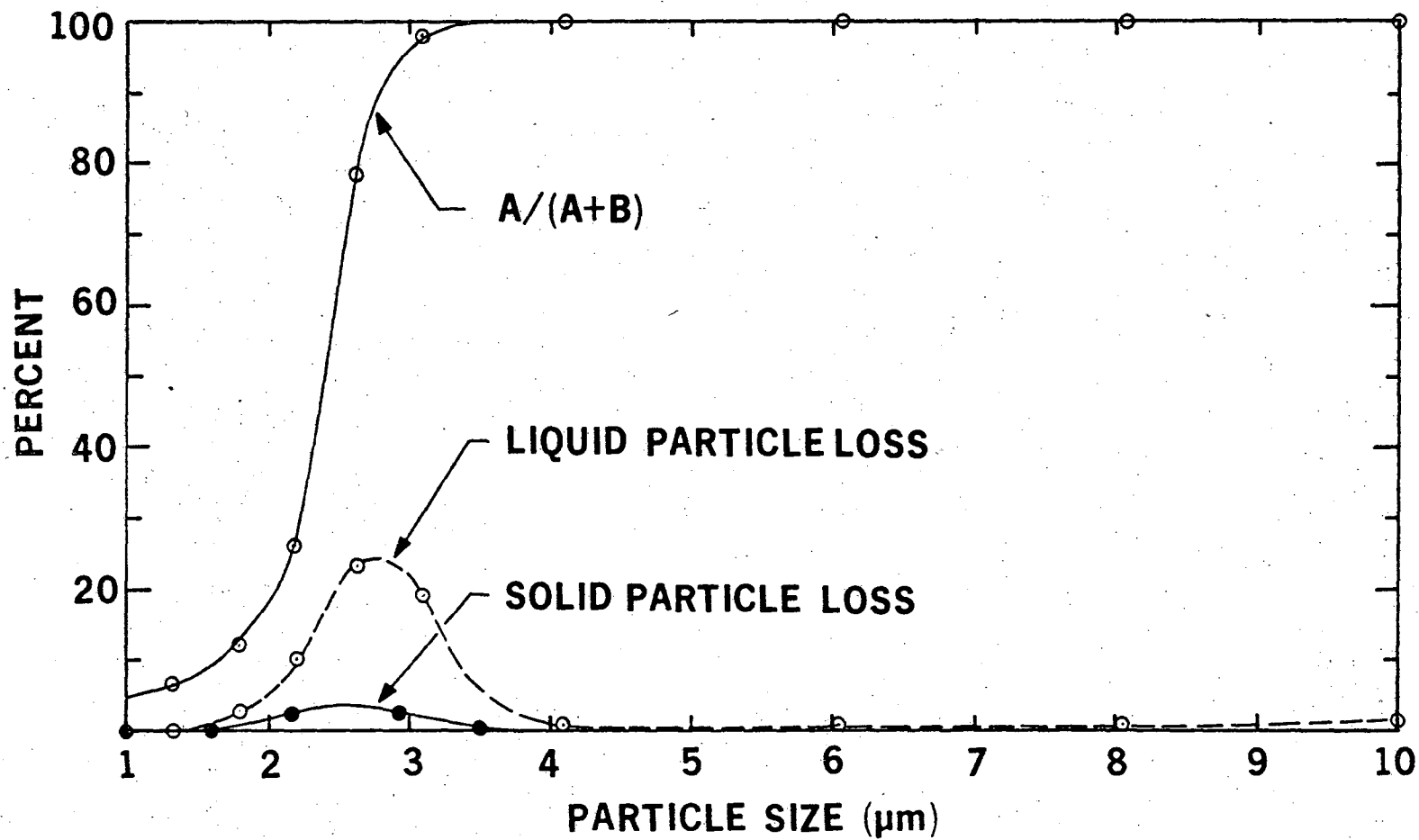
Figure 8. Particle size cut characteristics and particle loss
           measurements for the dichotomous sampler.

Figure 9. Photon excited energy dispersive analysis spectrum of a
           membrane filter containing the small particle fraction.
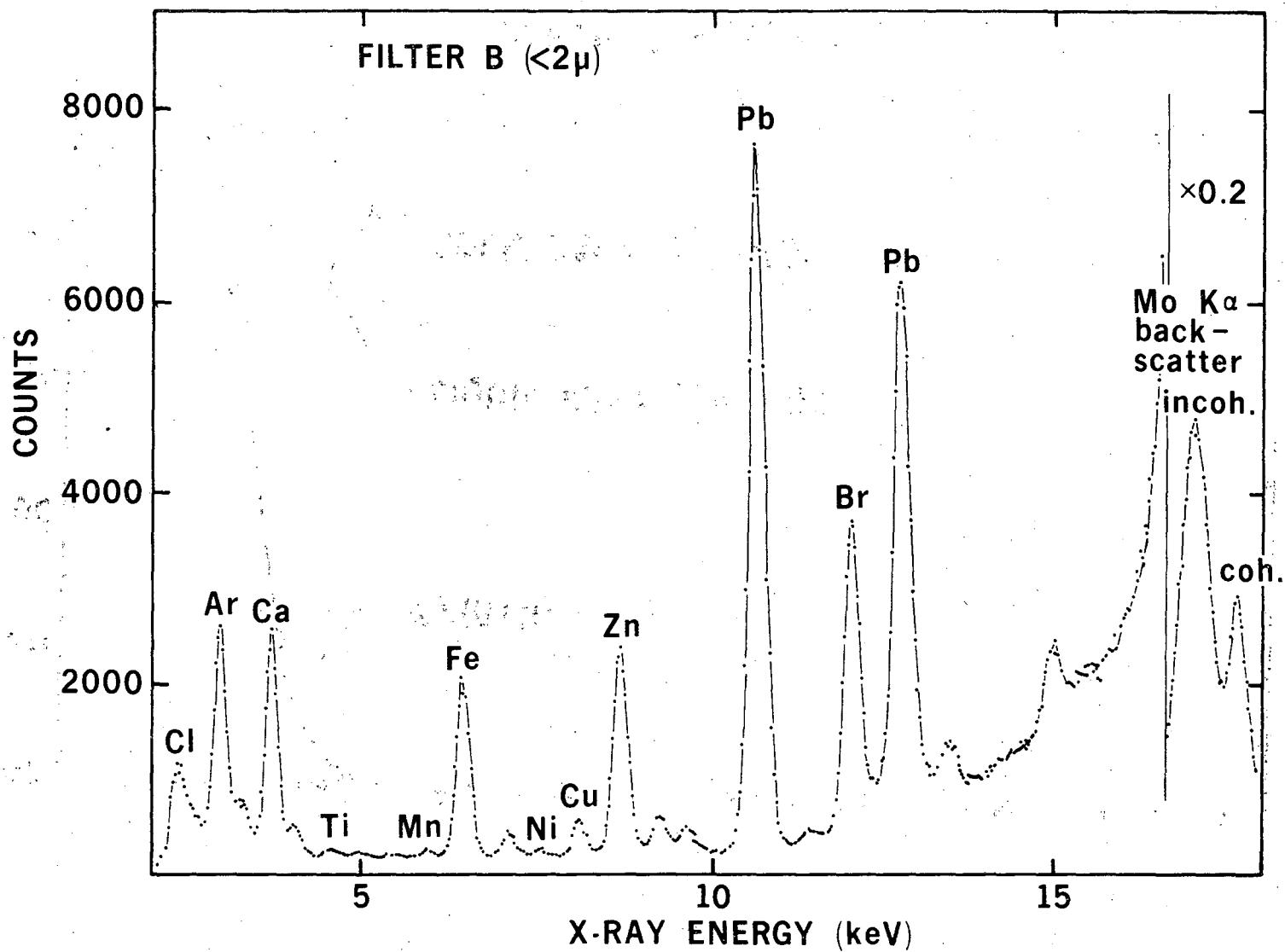
Figure 10. Photon excited energy dispersive analysis spectrum of a
            membrane filter containing the large particle fraction.

Figure 11. S and Pb concentration as a function of time for an
            urban sampling site.

Figure 12. S and Pb concentration for the complete network of
            stations averaged over the three day sampling period.

PRIMARY
RADIATION

SAMPLE

INCIDENT
PHOTON

EJECTED
ELECTRON

FLUORESCENT
X-RAY

CHARACTERISTIC
FLUORESCENT
X-RAYS

K

L

M

DETECTOR
SPECTROMETER

(a)

(b)

XBL 733-287

-12-

LBL-4834

Figure 1. Schematic of the X-ray fluorescence technique.

Figure 2.   The response of the spectrometer for monoenergetic photons striking the sample. The matrix is assumed to be composed of light elements.

SAMPLE HOLDER
WITH FILTER

X-RAY TUBE

W Anode

Collimator

SECONDARY TARGET

Ta Shielding

Electron Beam

Ta Shielding

Al Shielding

4mm

6mm
diameter

3mm depth

DETECTOR

0   1   2   3

SCALE: Inches

Figure 3. Sample — Fluorescer — Detector geometry employed in the
secondary fluorescence mode of energy dispersive analysis.

XBL 731-102
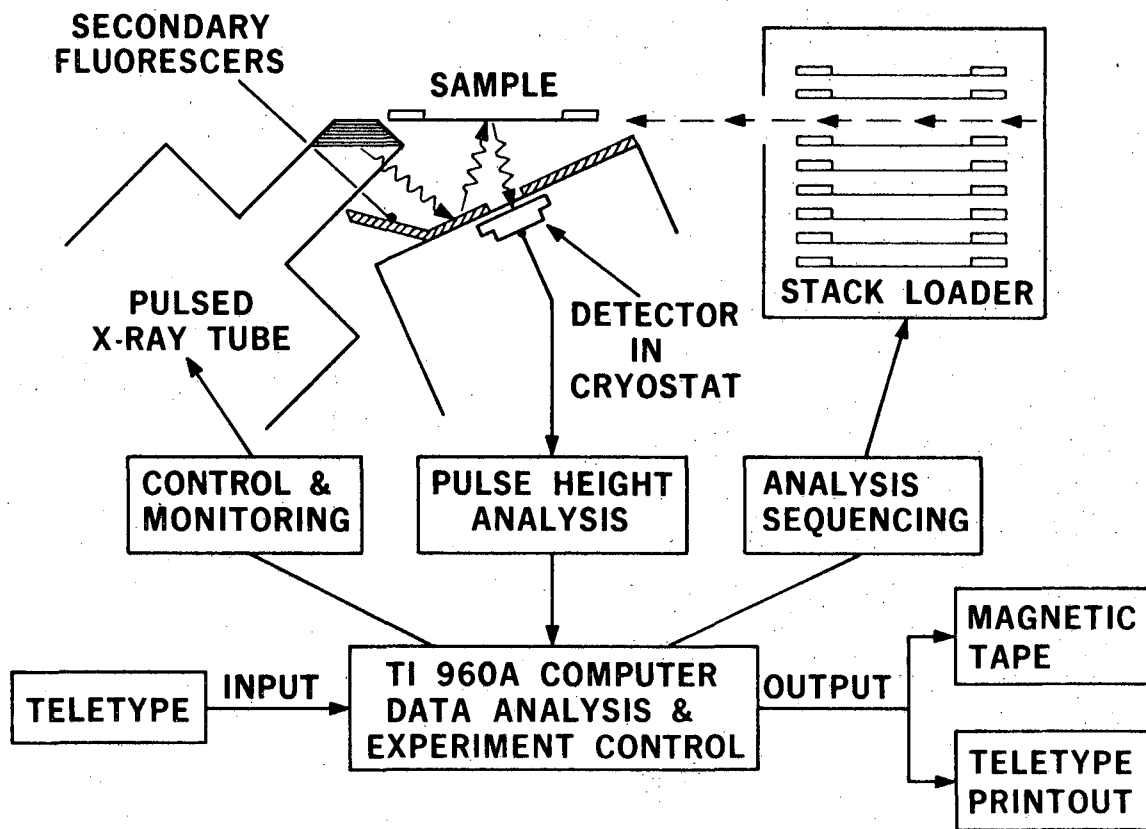
Figure 4.   Block diagram of complete analysis system.
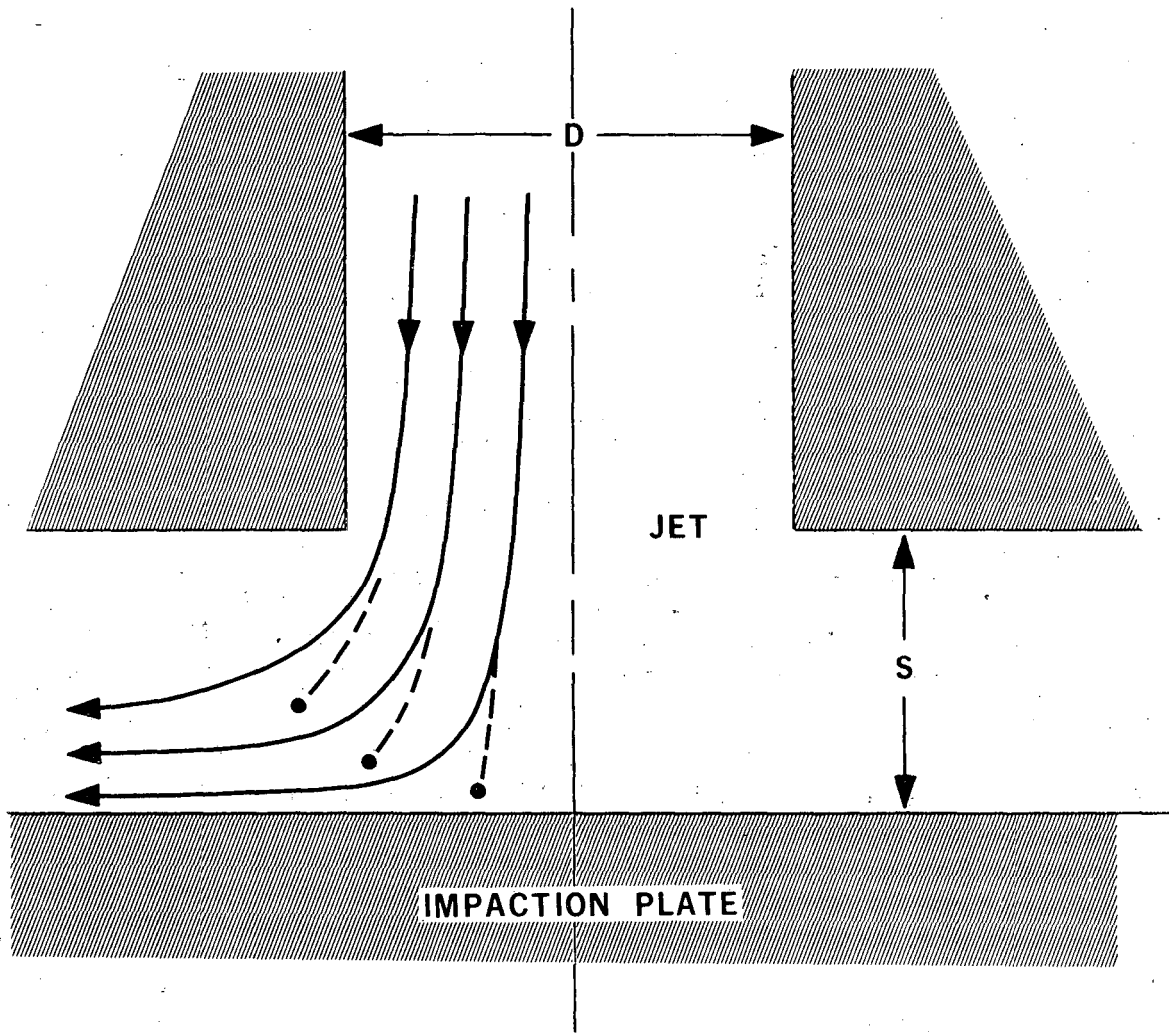
XBL 7411-8543

Figure 5.   Schematic of a single impactor stage.

XBL 746-1019

Figure 6. Schematic of a virtual impaction orifice.

FILTER A
(>2μm)

Q_0

P_1

FILTER B
(<2μm)

Q_1

Q_2

P_2

FLOW
LIMITING
ORIFICE

FLOW
MONITOR

CONTROL
VALVE

TO PUMP

XBL 746-1020

Figure 7. Flow diagram for a dichotomous virtual impactor.
Filters A and B are membrane type filters.

Figure 8.   Particle size cut characteristics and particle
loss measurements for the dichotomous sampler.

Figure 9.   Photon excited energy dispersive analysis
spectrum of a membrane filter containing the
small particle fraction.
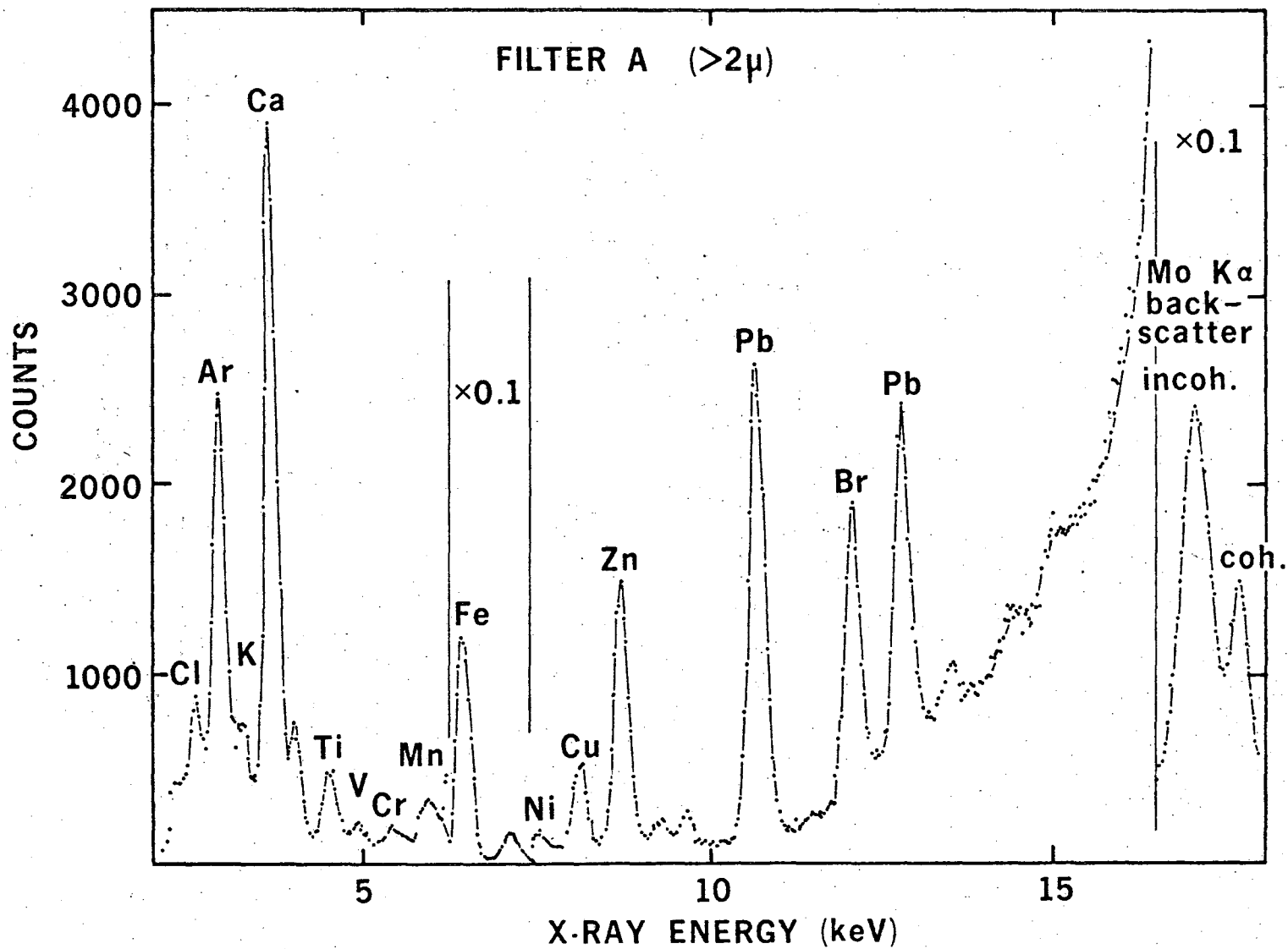
XBL 7411-8527

Figure 10. Photon excited energy dispersive analysis spectrum of a membrane filter containing the large particle fraction

XBL 7411-8526
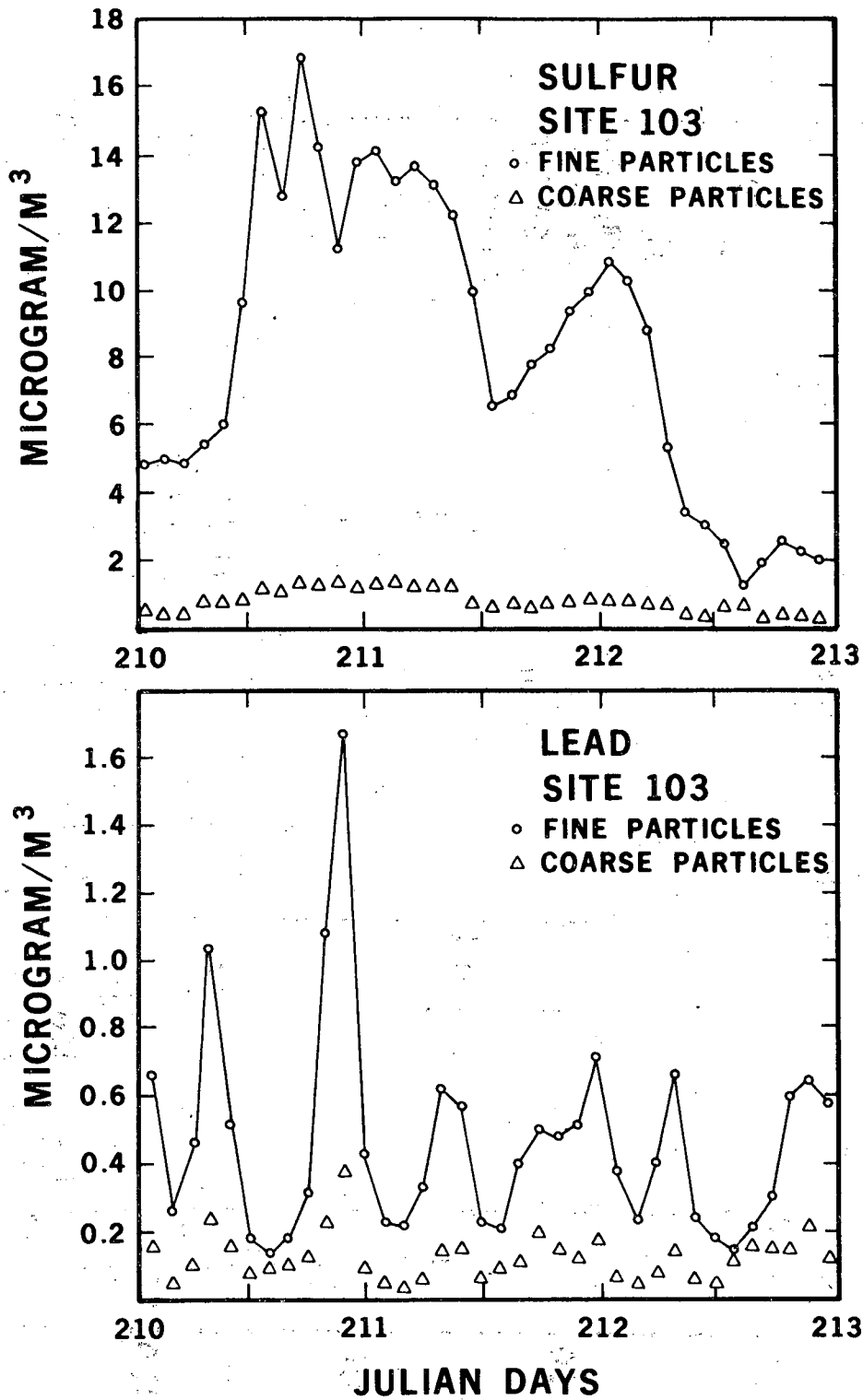
Figure 11. S and Pb concentration as a function of time for an urban sampling site.

XBL 763-656
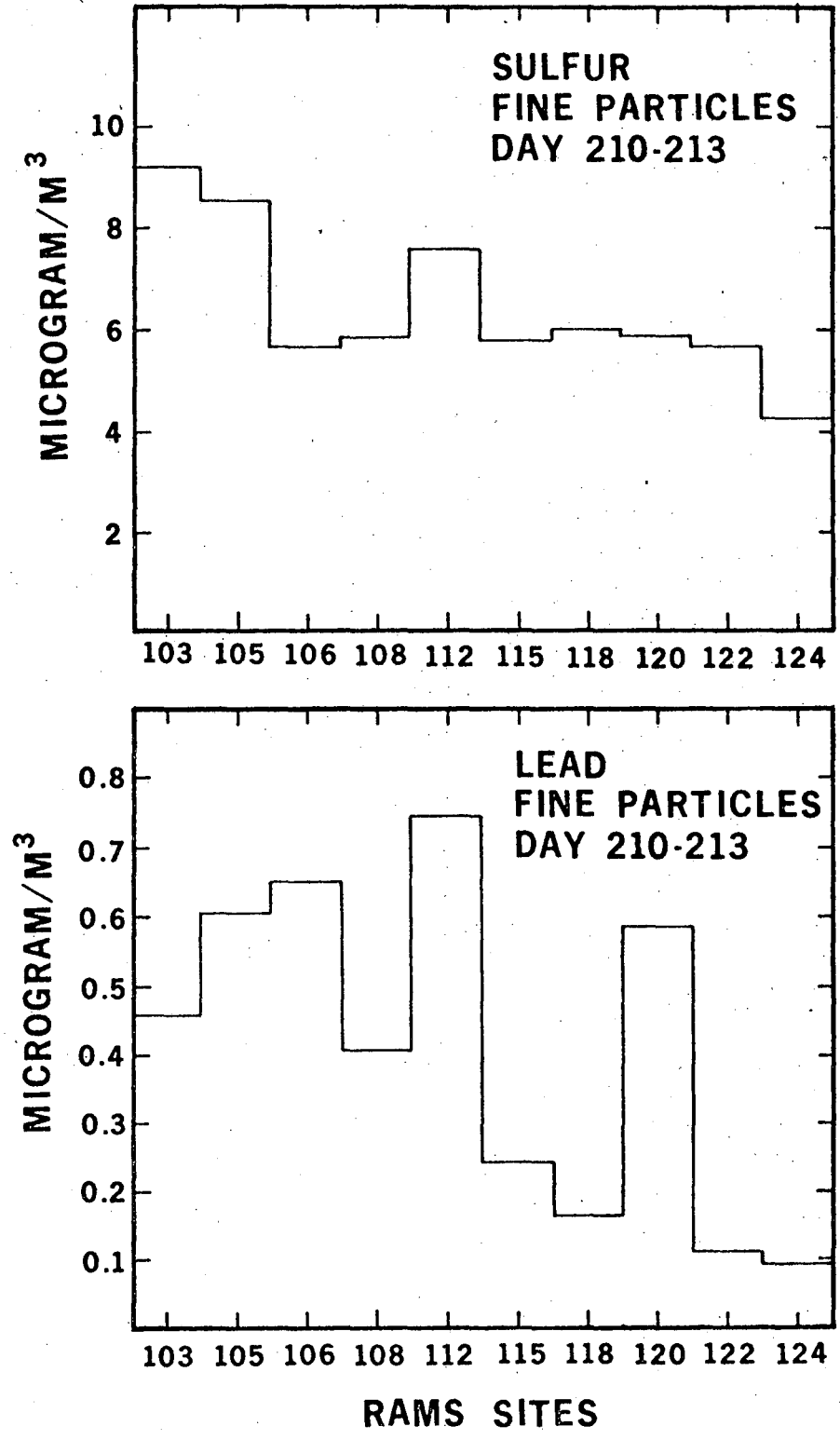
XBL 763-657

Figure 12. S and Pb concentration
            for the complete network
            of stations averaged over
            the three day sampling period.